Copyright Warning & Restrictions

The copyright law of the United States (Title 17, United States Code) governs the making of photocopies or other reproductions of copyrighted material.

Under certain conditions specified in the law, libraries and archives are authorized to furnish a photocopy or other reproduction. One of these specified conditions is that the photocopy or reproduction is not to be "used for any purpose other than private study, scholarship, or research." If a, user makes a request for, or later uses, a photocopy or reproduction for purposes in excess of "fair use" that user may be liable for copyright infringement,

This institution reserves the right to refuse to accept a copying order if, in its judgment, fulfillment of the order would involve violation of copyright law.

Please Note: The author retains the copyright while the New Jersey Institute of Technology reserves the right to distribute this thesis or dissertation

Printing note: If you do not wish to print this page, then select "Pages from: first page # to: last page #" on the print dialog screen

ABSTRACT

FORMATION OF BRANCHING ANGLES AT BIFURCATIONS OF ANT TRAIL NETWORKS

by
Subash Kusum Ray

Ants form dendritic trail networks around the nest to search for and exploit food sources located at the periphery of the network. Studies found these trail networks to be very efficient for the ants in terms of time and energy, which later was found stored in the bifurcation angle (θ) of the branches of these trail networks. It has been observed, that bifurcations are symmetrical when moving from the nest to the food source, while are asymmetrical when moving back towards the nest. The mean bifurcation angles have been found to be 50° - 80° for networks radiating out from the nest. This thesis focuses on the formation of the bifurcation angles and devising a model to illustrate their formation. It has been hypothesized that if the θ is small, the ants continue moving straight in the initial direction, and make the choice for an emerging branch after the bifurcation, thereby increasing θ, whereas it would decrease for large θ values, as the ants turn early to their choice of emerging branch. Also, for large θ values, it will be difficult for the ants to follow the trail. To test this, experiments with multiple individual ants were conducted on chemically marked 'Y' shaped paper strips with differing θ. Similarly in a model, simulated ants were run on 'Y' shaped trails with differing θ. Results show that the decision point (point at which ants turns for its emerging branch) moves away from the emerging branches with an increase in angle of bifurcation and the average maximum distance increases with the angle of bifurcation. Angles in the range of 20 °-60° were found to minimize the above constraints, and provide a stable trail network.

FORMATION OF BRANCHING ANGLES AT BIFURCATIONS OF ANT TRAIL NETWORKS

by
Subash Kusum Ray

A Thesis
Submitted to the Faculty of
New Jersey Institute of Technology
in Partial Fulfillment of the Requirement for the Degree of
Masters in Biology

Department of Biological Sciences

August 2014

APPROVAL PAGE

FORMATION OF BRANCHING ANGLES AT THE BIFURCATIONS OF ANT TRAIL NETWORKS

Subash Kusum Ray

Dr. Simon Garnier, Thesis Advisor — Date
Assistant Professor of Biology, NJIT

Dr. Claus Holzapfel, Committee Member — Date
Associate Professor of Biology, Rutgers - Newark

Dr. Jessica Ware, Committee Member — Date
Assistant Professor of Biology, Rutgers – Newark

BIOGRAPHICAL SKETCH

Author: Subash Kusum Ray

Degree: Master of Science

Date: August 2014

Undergraduate and Graduate Education:

- Master of Science in Biological Sciences,
  New Jersey Institute Of Technology, Newark, NJ, 2014

- Bachelor of Technology in Biotechnology,
  The ICFAI Institute of Science & Technology, Dehradun, India, 2012

Major: Biology

This thesis is dedicated to my Maa and Baba, without their support
I wouldn't have reached here.
To my Dada, his constant encouragement helped me
through the low moments.
And my friends Souvik, Swayam, Shazia and Rashmita
who helped to keep up a smile while at work.

ACKNOWLEDGEMENT

I would like to thank Dr. Simon Garnier my thesis advisor who has been a guiding light throughout and without whose support this thesis would have never been possible. It has been an invaluable opportunity for me to work at 'The Swarm Lab' at NJIT under his direction.

I would also like to thank my thesis committee members, Dr. Claus Holzapfel and Dr. Jessica Ware for their support and guidance.

My special thanks to Dr. Chris Reid, his timely suggestions helped me make this a better project.

I would like to thank my friends Souvik, Swayam, Rashmita and Shazia for their constant support in my studies. My sincere appreciation goes to my lab mates Nidhi, Courtney and Osvaldo. Their time to time help has helped me make this project better.

Last, but not the least, I would like to thank my family for their immense support throughout.

TABLE OF CONTENTS

TABLE OF CONTENTS
(Continued)

Chapter **Page**

LIST OF TABLES

LIST OF FIGURES

LIST OF FIGURES
(Continued)

LIST OF FIGURES
(Continued)

LIST OF FIGURES
(Continued)

CHAPTER 1

INTRODUCTION

1.1 Background Information

Ants are social insects that are found running through much of the terrestrial world (except Antarctica, Greenland and Iceland). Their biomass exceeds all vertebrates when combined [1]. The ecological success of ants is also well illustrated in terms of diversity with known living ants comprising 11 subfamilies, 297 genera, and 12,000 species under family Formicidae [1]. Ants form highly structured eusocial nest colonies which consist of a fertile queen (or queens) that lays eggs, and infertile female workers which forage for food, care for the queens offspring (brood), work on the nest, protect the community (in this task they are known as soldiers), and perform many other tasks. Colonies also produce a fertile male ant at certain times of the years that dies soon after mating. Colonies may or may not have strong physical differences separating the queens and worker castes. Ant colonies operate as unified entities, working for the nest together and thus described as superorganisms [2]. Ant colonies work without central control, with each ant playing a bit part role towards the nest. Individual ants react to information from the local environment and thus, interact following a simple set of rules. Various complex collective behaviors emerge as a product of the interactions between many individuals, making an ant colony a self-organized system with no ant or individual having universal knowledge of the colony needs.

Some ant species produce large dendritic patterns of pheromone trails around their nest to move and navigate in the foraging area to searching for and exploiting various food sources[1,3]. These trails start from the nest as thick ‘trunk’ trails, which

split into thinner branches and die off with increasing distance from the nest. Such pheromone trail networks are formed by individuals following a simple set of rules. The trails are formed as a result of successive pheromone deposition, first by a scout (forager) that discovers the food source and returns to the nest, then by workers who are recruited by these scouts as a result of strong positive feedback provided by recruitment pheromones. Trail formation in ants is a self-organized process based on the interplay between a positive feedback (reinforcement of the trail by the recruited ants) and a negative feedback (pheromone evaporation). Ant foraging trail networks are among the most important examples of transportation networks in animals without central control.

Various studies on ant trail networks have shown that bifurcations in the dendritic trails hold a key to help an ant make adaptive decisions like choosing the shortest path to its destination, and this information was later found to be stored in the geometry of the trail bifurcations [4-7]. The mean bifurcation angle of the emerging branches have been observed to be between 50°- 80° as they radiate out from the nest (*Atta sexdens*, *A.capiguara*, *A.laevigata*, and *Messor barbarous* = Acosta et al.(1993) [4]; *Monomorium pharaonis* = Jackson et al. (2004) [8]; *Formica aquilona* = Buhl et al. (2009) [9]). The bifurcations were such that an ant travelling towards the periphery of the nest heading for the food source (foodbound or outbound ant) encounters symmetrical bifurcations, i.e., the two emerging branches deviate at equal angles from the bifurcation (deviate at ~30°). Likewise, ants travelling back to the center of the network (nestbound or inbound ants) encounter asymmetrical bifurcations. At the asymmetrical bifurcation one emerging branch deviates less (~30°), and the other branch deviates more (~120°) from the initial direction of travel. The branch deviating less leads the ant towards the nest, and the

branch deviating more leads it back to the periphery (away from the nest). This bifurcation geometry helps create an intrinsic bias or polarity in the bifurcation even in the absence of pheromone as the ant chooses the less deviating branch at an asymmetrical bifurcation [5-8]. The trail geometry also helps the ants to orient and navigate in space such that they reach their intended destination (i.e., towards the food source or towards the nest) with minimum cost involved in terms of time and energy [5,6,8].

Jackson et al. (2004) [8] experiments on *Monomorium pharaonis*, showed that an unfed ant will generally encounter a symmetrical bifurcation (as unfed ants are foodbound, and the network bifurcations are symmetrical when radiating out from the nest to the food source). However, when the unfed ants encounter an asymmetrical bifurcation, they have a high tendency to make a U-turn, and thus return back to the point of departure. This behavioral pattern helps the unfed ants to reorient themselves on the trail, as encountering asymmetrical bifurcations means the trail is leading it towards the nest. Similarly, fed ants which generally encounter asymmetrical bifurcations (fed ants are nest bound, and the bifurcations are asymmetrical when returning back to the nest) make U-turns when facing symmetrical bifurcations because encountering symmetrical bifurcations means the ant is on its way back to the food source. Therefore, *Monomorium pharaonis* ants use the geometry of the bifurcation to orient themselves correctly within the network, thereby saving time and energy. In Argentine ants *Linepithema humile*, Gerbier et al. (2008) [6], used artificial gallery networks to show that workers that return to the nest with food and reach an asymmetrical bifurcation preferentially select the less deviating exit (emerging) branch and perform more U-turns on the branch that deviates more. As a consequence, the least deviating path would be marked with a greater amount

of pheromone and would more likely be selected by the ants. Since, the less deviating branch leads towards the nest, an Argentine ant colony will choose a more direct or the shortest path back to its nest. In another study by Garnier et al. (2009) [5] on Argentine ants, the global behavior of ants was examined in an experimental arena of polarized and non-polarized bifurcations. A polarized arena is similar to a natural setup where outbound ants face symmetrical bifurcations and inbound ants face asymmetrical bifurcations, whereas a non-polarized arena is an arena with only symmetrical bifurcations for both outbound and inbound ants. It was found that ants spent less time on the shortest path and dispersed more in the non-polarized arena, thus resulting is reduced overall performance of the colony as pheromones were laid almost uniformly in the whole arena. This demonstrated the importance of structural properties on the efficiency of ant transportation networks.

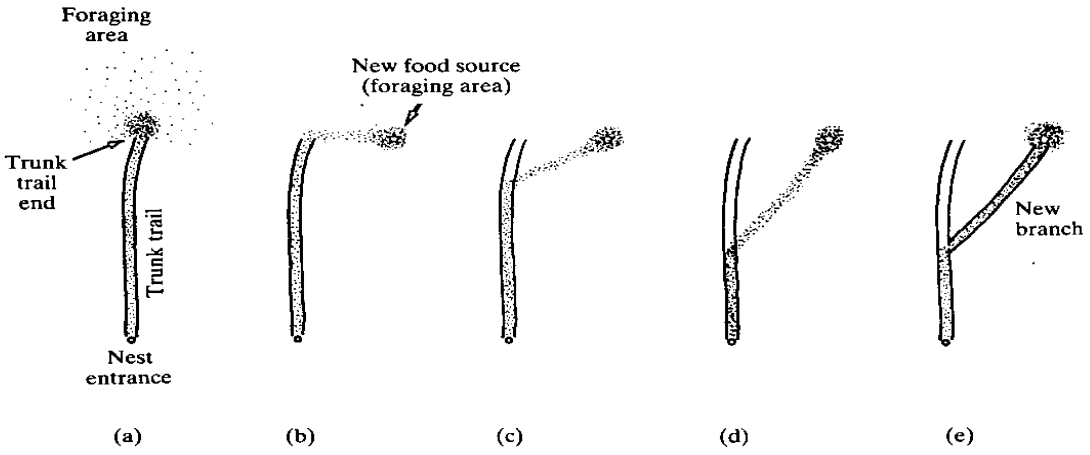

Figure 1.1 Shows the hypothesized steps of formation of trunk trails as postulated by Acosta et al. [4] a) Initially ants follow the trunk trail from the nest to the foraging area; b) A new food source is found by a scout to which the column of foraging ants first travels to the end of the trail, and then turns towards the food source (following the pheromone trail); c – d) the column of foragers changes its distance gradually to arrive at trunk trail; e) if the newly discovered food source remains long enough, it's exploitation becomes intensive and a new branch is constructed which reaches an angle of confluence with the trunk trail [4].

Previous studies were mainly focused on the structure of the networks and the way ants behaved in these networks at both the individual and the collective level, but a question still remained unanswered: how do ants form such efficient trail networks despite their limited cognitive abilities? This study intends to shed light on the probable mechanisms involved at the individual and collective level in the formation of the bifurcation angle of these trail networks. This thesis elaborates the postulate made by Acosta et al. (1993) [4] that if a newly discovered food source is placed laterally with respect to the trunk trail, the path used by the ants changes progressively towards the direction of the nest entrance until reaching a certain angle of confluence between the chemical and trunk trail (Figure 1.1).

This study hypothesizes that if an ant encounters a bifurcation with a small angle between the emerging branches (θ, angle of bifurcation), the ant will continue moving straight on the initial traversed path for a while even after the bifurcation. This is because the ants face difficulty in differentiating between the two branches because, i) the emerging branches deviate at small angles, and thus seem like the initially travelled path itself, and ii) since, the two emerging branches are close to each other, the branches seem to be running together as the diffusive nature of pheromone creates a smudge area between the two branches just after bifurcation. Therefore, an ant makes a late turn on its choice of branch. With subsequent ants turning late and with pheromone evaporating with time, a new trail is laid with the bifurcation point shifted towards the emerging branches and a larger bifurcation angle.

Conversely, if an ant encounters a bifurcation with a large angle (θ) between the emerging branches, the ant will have difficulty following one or the other emerging

branch. The difficulty is mainly caused by the inability of the ant to make sharp turns towards one of the branches at the bifurcation. With subsequent ants following the same behavior and with pheromone evaporating with time, the shift in bifurcation point will be towards the initial branch. Also, as the ants fail to follow the trail at the part of the network around the bifurcation, the chances of ants losing the trail increases.

This study summarizes a set of intermediate angles, where i) this increase and decrease in bifurcation angles reaches equilibrium, and thus provide a stable network structure, and ii) makes the trail accessible for the ants to follow at all positions (i.e., before and after the bifurcations).

CHAPTER 2

MATERIALS AND METHODS

2.1 Biological Material

Colonies of the Argentine ant *Linepithema humile* (Formicidae, Dolichoderinae) were collected on the campus of the University of Toulouse, France. Ants were housed in artificial plaster nests, reared in an experimental room at constant temperature of 80° F under constant light conditions (L:D 12:12) and fed *ad libitum* with a mixture of eggs, carbohydrates and vitamins [10], as well as *Musca domestica* maggots. Twelve groups containing one thousand workers each, no queen and no brood were counted about one week prior to the experiments and placed in separate nests 10 cm in diameter, connected to a small foraging arena also 10 cm in diameter. Groups were starved for 24 hours before each experiment to stimulate exploratory behavior.

2.2 Experimental Setup and Protocol

The experimental setup consists of a circular arena (Figure 2.1) of diameter 20 cm, which is an enclosure with walls covered with Fluon®. Fluon covering makes the wall smooth, which weakens the grip of the ants on the wall surface, making it difficult to climb and escape the arena. The floor of the arena was covered with a sheet of chlorine free paper, which was replaced after each experiment such that the arena was clean of any previously laid pheromones. The entire setup was surrounded with white homogenous curtain to eliminate as many orientation cues as possible. In the middle of the arena a 'Y' shaped pheromone paper strips were laid, on which individual experiments were conducted. 'Y' shaped strips were constructed by rearranging pieces of paper on which a fresh chemical

trail had been deposited. The pieces of paper were marked with chemical pheromone, by allowing workers of a colony of the *L.humile* to travel between the nest and a food source (1-M sucrose solution) for 30 minutes. This duration ensured that the paper was marked homogenously and the strips were saturated with pheromone. The trail pheromone duration of *L.humile* is estimated to be close to 30 min [11]. To avoid the effects of trail decay, the same pieces were used during 20 minutes only for each experimental replicate. The paper strips were 1cm wide, 8 cm long for the emerging branches, and 5 cm long for the initial branch that extends out from the start chamber (ϕ = 2cm). Individual behaviors of ants were tested in a series of experiments conducted on the chemically laid 'Y' shaped pheromone strips with differing angles of bifurcation (θ; i.e., the angle between the emerging branches**,** Figure 2.1). The angles of bifurcations (θ) considered for the experiments were 30°, 60°, 90°, 120 °, 150° and 180°. No food sources were present in the arena at any time.

Tests started by allowing one starved ant to climb spontaneously on a wooden skewer from its nest box. The skewer was then gently moved towards the testing area so as to minimize disturbance of the ant's behavior. The ant was then allowed to climb down the skewer at its own convenience into the start chamber (Figure 2.1). Each ant was allowed to move on the marked 'Y' shaped paper strips and was then taken off after it reached the tip of the chosen emerging branch. The ants once used were kept separately and not used again in any of the following experiments. Experiments for a particular angle of bifurcation (θ) were performed in two sets of 20 minutes each (i.e., the time before the trail starts decaying). 70-80 runs were done for each experiment. The possibility of ants perceiving the pheromone trails laid by ants during previous runs of the

experiment were nullified as the strip of paper used were already saturated with pheromone. The experiments were filmed by Canon EOS 20D camera at 25 frames per second and 640 X 320 pixel resolution.

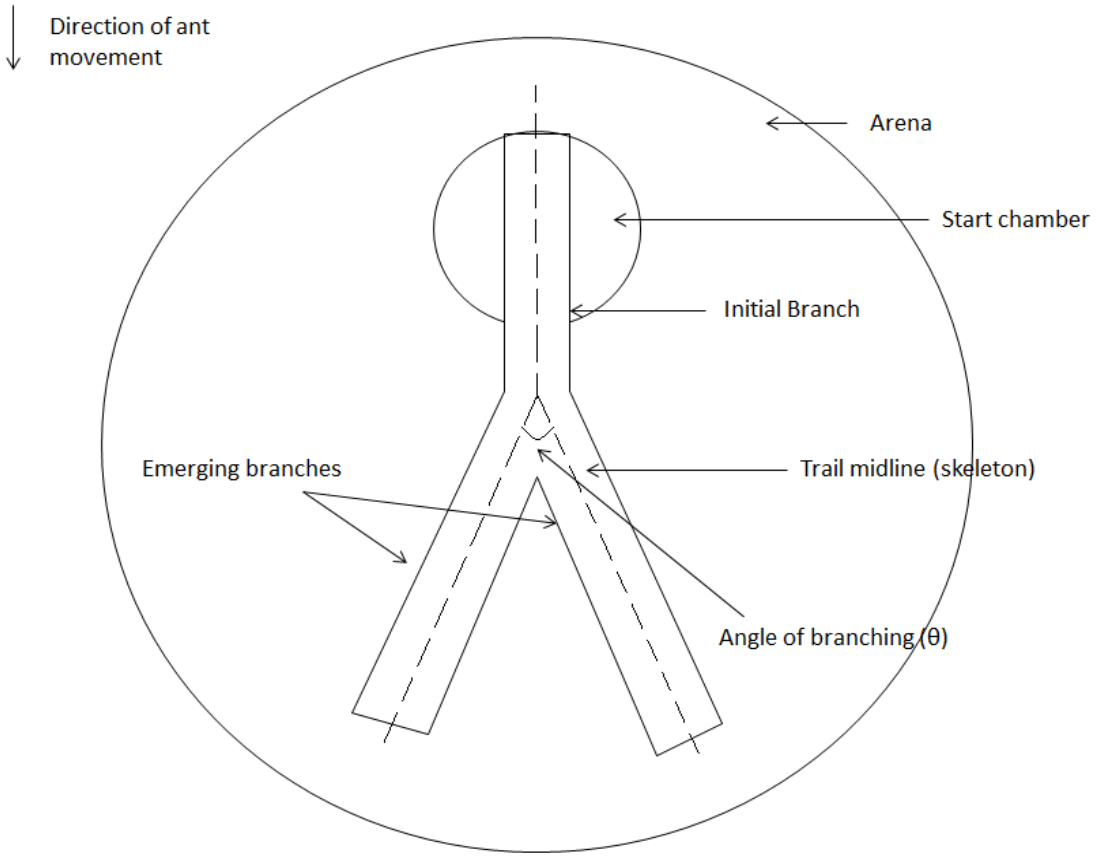

Figure 2.1 The arena for the experiments. The angle of branching (θ) was altered between treatments (30°, 60°, 90°, 120°, 150° and 180°). The ants were initially introduced in the start chamber, from where they followed the 'Y' trail until the end of an emerging branch chosen at the bifurcation. The whole arena was an enclosure with wallsa covered with Fluon® to prevent ant escape. The trail midline was found by the Image Processing toolbox in MATLAB®.

The filmed videos of each experiment were saved in MOV format. Video excerpts of each run were extracted and stored in separate folders belonging to the experiment with the particular bifurcating angle. Video excerpts were extracted in mpeg – 4 format

using iMovie®. Each video excerpt started with an ant in the start chamber, from where it moved on the 'Y' shaped paper strip until it reached the tip of an emerging branch (which it chose at the bifurcation). This video excerpt was later used for finding the trajectory of ants in each run. Coordinates of the ant trajectories from the video excerpts were produced using SwisTrack® (explained in detail in Section 2.3.3). Another video excerpt containing the empty arena before each run was extracted (i.e., from the part when the ant from the previous run was removed and the ant from the next run was prepared). From this excerpt the background or reference images for each run were produced. This was done using program called Backgrounder® (explained in detail in Section 2.3.1).

2.3 Software Tools for Data Extraction and Protocol

2.3.1 Extracting Background Image Using Backgrounder®

Backgrounder® is a program used to extract reference images from a video. It was used to find the background image before each run of experiment (i.e., before the ant was introduced into the arena). The background image used in this analysis was the median of all image frames of the excerpt with no ant in the arena. Backgrounder® stacks all the image frames onto one another, and then computes the median pixel for each pixel coordinate. The image formed from the median pixel for every pixel coordinate is the background image. The image was exported in Portable Network Graphics or .png format.

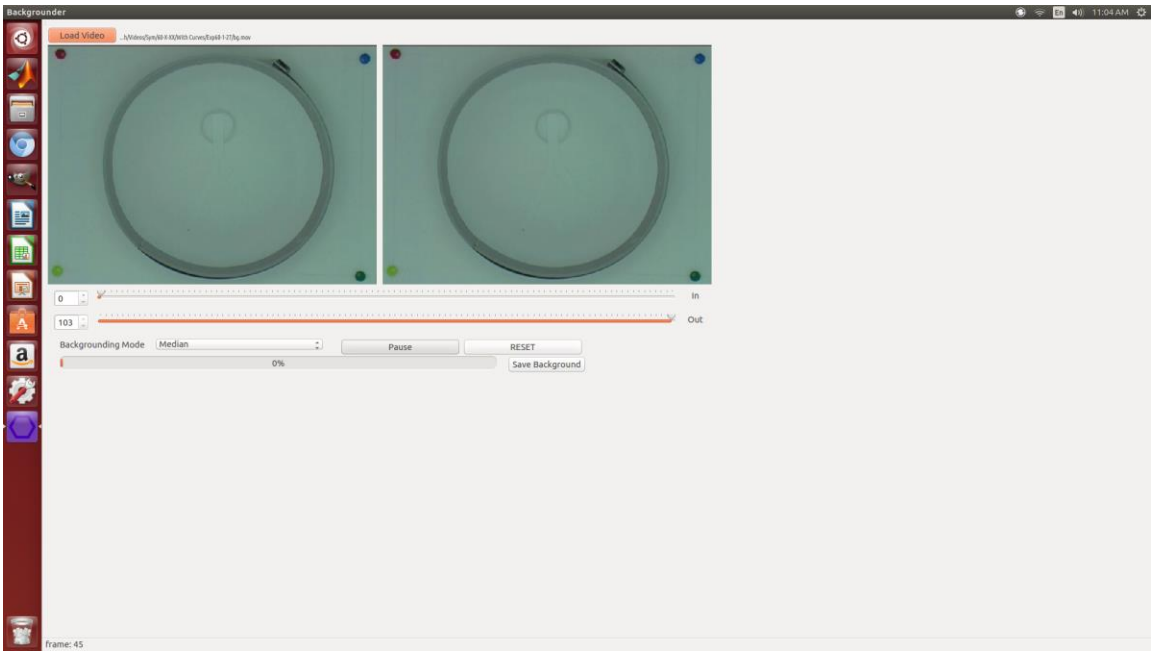

Figure 2.2 Computer screenshot of Backgrounder®. First the video excerpt without the ant was loaded using the 'Load Video' button, then backgrounding mode 'Median' was selected in the scroll down menu. The software stacked all the frames of the video together on the left midsection of the software interface (as seen in the figure), and the resulting median image was produced on the right midsection.

The median image was preferred over the mean because the median is the least sensitive to variations in the outlier values. The interface of the software is shown in Figure 2.2**.** The background image acted as a reference to the image frames in the video excerpts containing the run.

2.3.2 Extracting Image Trail and Image Mask using GIMP®

GIMP (GNU Image Manipulation Program) is an open source graphics editor used for image retouching and editing. GIMP® was used to create an image 'mask' (Figure 2.3a) i.e., an image that contained the whole arena (part where experiments were conducted), and a 'trail' image (Figure 2.3b) i.e., the Y-shaped chemical strip. The image mask ignored areas that were not a part of the experiment (used in SwisTrack®, in detail in

next section). The image trail was used for data analysis (extracting the midline of the trail for analysis of ant trajectories). The images were exported as binary images such that the inner relevant areas were represented by white pixels, and the outside ignored area were represented by black pixels (Figure 2.3 a and b). These images were extracted from the background image and saved in Portable Network Graphics or .png format.

a) 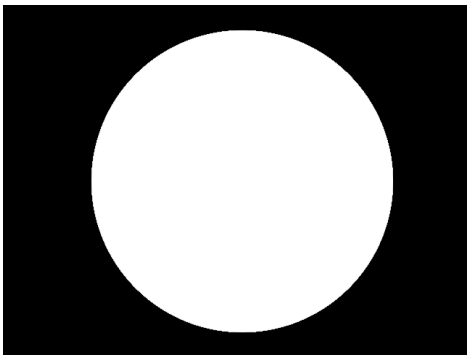 b) 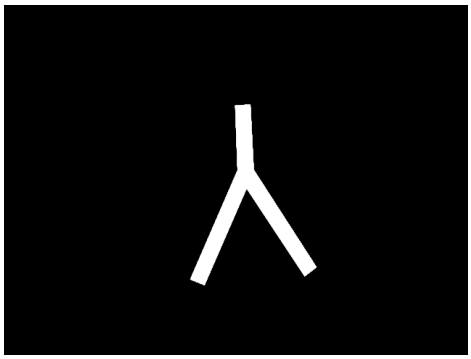

Figure 2.3 a) Image Mask, which helped ignore the irrelevant areas for data analysis. The circular arena in the background image was first outlined, and then the inner part of the arena (relevant area) was colored white, and the outer area (irrelevant area) was colored black. b) Image trail, was used for data analysis (explained in later sections). The inner part of the trail (i.e., the part which was chemically laid) was colored white and the rest was colored black.

2.3.3 Extracting Ant Trajectory Using SwisTrack®

SwisTrack® was used to produce trajectories of ant movements in each run of experiments. The program gives the pixel coordinates of an ant in each frame of the run video (excerpt), which when joined or plotted gives the overall trajectory. SwisTrack is a flexible open source tracking software used for multi – agent systems. It is a powerful tool used for tracking robots, humans, animals and objects using camera or a recorded video as input source [12]. It uses Intel's OpenCV library for fast image processing and contains interfaces for USB, FireWire and GigE, as well as AVI files [12].

Figure 2.4 shows the Graphics User Interface (GUI) of the software. The software architecture is component-based, where each component performs a particular task and conforms to interact with the other components in the sequence (Figure 2.4). Components interact by passing their data through structures referred as 'data channels'. The data channels shown in Figure 2.5 are: *input, grayscale image, color image, binary image, particles, and tracks*. Each component reads (R), edits (E) or writes (W) any of these data channels (Figure 2.5). The components are assembled by the user such that the data channels read by any given component has been previously been written (W) by another component. SwisTrack classifies the components into ten categories, and proposes a certain order in which the components should be executed (following the processing pipeline; Figure 2.6). The processing pipeline (Figure 2.6) models the components considered for extracting ant trajectories (Figure 2.4). The output image as result of processing by each component is as shown in Figure 2.4b. The description of the software and protocol is in the Figure 2.4 legend.

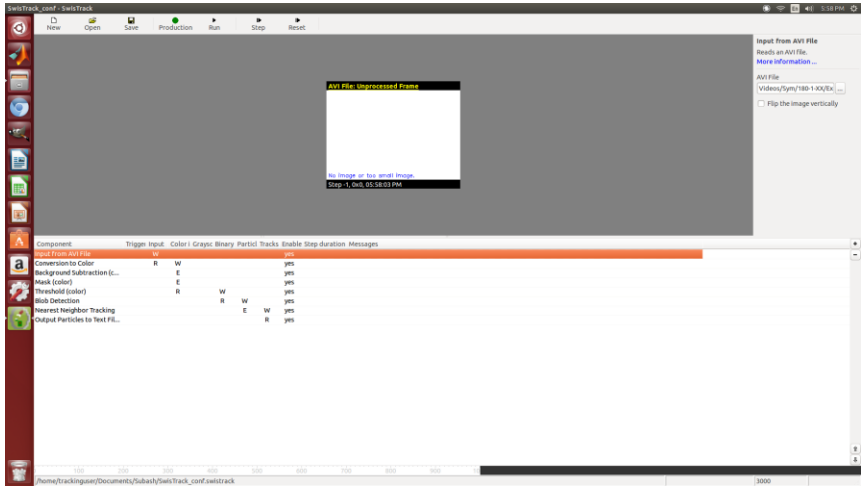

(i)

(ii)

(iii)

(iv)

(v)

Figure 2.4 a) Graphical User Interface of SwisTrack®. The main display is at the center. It displays the processed images after each step. The lower panel shows the components used. The left panel shows the controls and parameters associated with the component. **b)** Shows the processed image after each step of action by a component with **i)** Input video (unprocessed frame); **ii)** After background subtraction (subtracting the background image from each frame of the excerpt; white pixels in the middle is the ant); **iii)** Image after the application of mask (ignores the irrelevant area i.e., area outside of the arena). Mask reduces the possibility of finding a particle outside the arena; **iv)** Image after thresholding, such that the particle (which is ant) is well expressed; **v)** the blob detects the particle (ant); **vi)** Nearest neighbor tracking, where the software tracks the coordinates of the blob as it moves with the ant through the run.

Component	Trigger	Input	Color image	Grayscale image	Binary image	Particles	Tracks	Enabled	Step duration	Messages
Input from AVI File		W						yes		
Conversion to Color		R	W					yes		
Background Subtraction (c...			E					yes		
Mask (color)			E					yes		
Threshold (color)			R		W			yes		
Blob Detection					R	W		yes		
Nearest Neighbor Tracking						E	W	yes		
Output Particles to Text Fil...							R	yes		

Figure 2.5 The extreme left column shows the components used for extracting ant trajectories. Each components conforms with other components in the pipeline, where an image read (R) by one component should be written (W) by one of the previous components through the Data channels (all other columns after the first column).

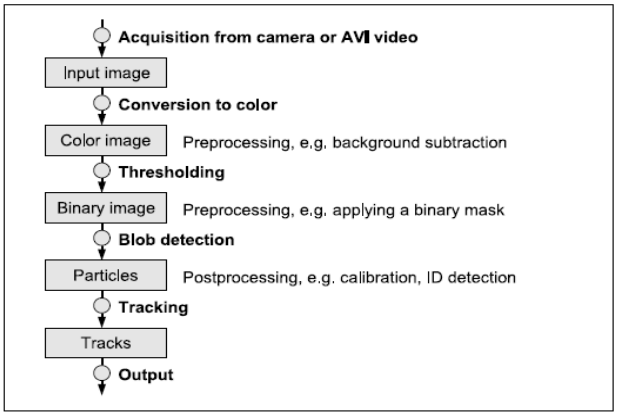

Figure 2.6 Standard processing pipeline of image processing in SwisTrack®. The order of components shown in Figure 2.5, was chosen following the processing pipeline.

SwisTrack® gives the pixels coordinates (X and Y) of an ant in each frame of the video excerpt as output. These pixel coordinates when plotted gives the trajectory of an ant in that particular run. Trajectories of all runs were extracted for analysis. The pixels coordinates can be plotted on the trail image using MATLAB® to see the trajectory of the ant in each run (Figure 2.7).

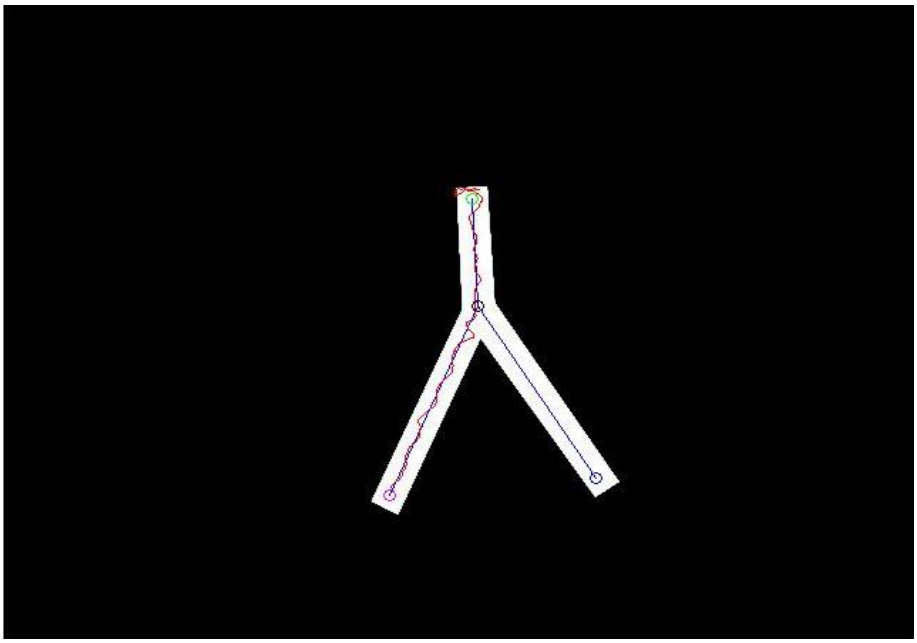

Figure 2.7 Ant Trajectory (in red) with θ = 60° plotted on the trail image. The blue line passing through the middle of the trail is the trail image midline (midline of the white pixels). The end coordinates of the midlines are marked by circles (o) with different colors (green – initial branch; magenta and blue – emerging branches and black where the midlines of the 3 branches meet, also known as the bifurcation point).

2.4 Model

In order to test our predictions, an agent-based model of ant trail following was developed. Simulated ants were run on 'Y' shaped trail model with pheromone, and differing angle of bifurcations between the emerging branches. The model is based on a recent study by Perna et al. [13] on *L.* humile. In this study, the authors found that the trail following behavior of an ant showed a Weber's Law response to the pheromone it lays while foraging for food (explained in detail in Section 2.5.3).

2.4.1 Body Specifications

In the model, ants were represented by a set of points (Figure 2.8) corresponding to the tip of the abdomen, the center of the body (used for tracking in the simulations), the head,

and the left and right antennae. The total body length (tip of the abdomen to head) is 3mm. The antennae are also 3mm long deviating at 45° to the right and left side of the head (Figure 2.8).

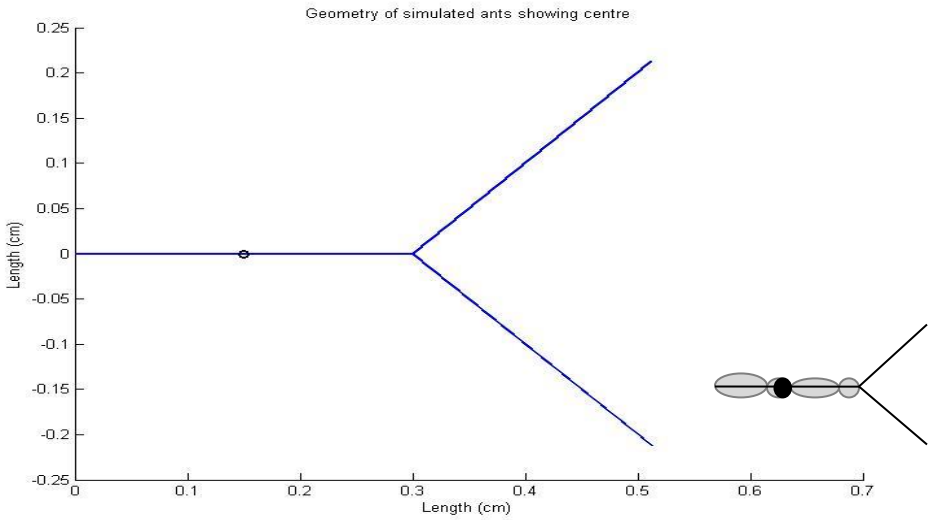

Figure 2.8 Simulated ant body specifications. The black dot in the center represents the body center (with respect to which simulations were tracked). Inset shows the fit of the simulated ant.

2.4.2 Spontaneous Movement

In absence of pheromone, ants move according to a correlated random walk. Ant movements were recorded for 40 ants in the circular arena (same arena as used for experiments i.e., in Figure 2.1) for two minutes in the absence of pheromone and the start chamber. The movements of ants in the random walks were characterised to define different parameters of the model for the simulations. Examples of a few extracted trajectories are shown below in Figure 2.9.

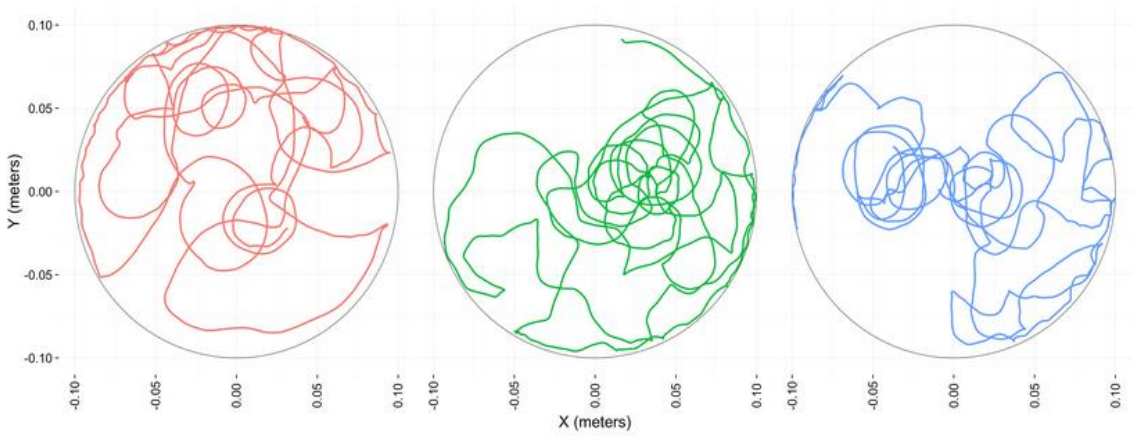

Figure 2.9 Trajectories of ants performing a random walk on the circular arena without any food source. The ants tend to align and walk with the wall, showing a thigmotaxis tendency.

2.4.3 Trail Following Behavior

As mentioned before, the trail following behavior of ants was modeled according to the findings in the study by Perna et al. [13]. The ant decision to turn towards the center of the pheromone trail followed Weber's law in the following form:

$$\propto = A\frac{L-R}{L+R} \tag{1.1}$$

where **α** is the angular speed that an ant adopts with pheromone **L** and **R** detected by the tip of the left and right antennae of the ant respectively. **A** is the maximum angular speed that an ant can adopt (this parameter was found by analyzing the trajectories from the random walks). The expression **(L – R) / (L + R)** is known as the 'Michelson Contrast' of the stimulus pattern. The ratio is of the type 'signal difference / average signal'. This relation does not depend on the specific scale used to measure pheromone, as the same

relation holds if **L** and **R** are both multiplied by the same constant. This even nullifies the effect of pheromone evaporation which decreases the pheromone quantity, as it can produces a result similar to multiplying both **L** and **R** by a constant smaller than one.

2.4.4 Pheromone

Pheromone intensity 'I' was given by:

$$I = \frac{Q}{2\pi D\tau} \exp\left(\frac{-r^2}{4D\tau}\right) \quad (1.2)$$

where **Q** is the amount of pheromone deposited (g cm^{-1}) at a radial distance **r**, with diffusion coefficient **D** (D = 0.01 cm^2s^{-1}, approximating the typical diffusion constant of trail pheromone [14-16]). Tau **τ** is the diffusion time of the pheromone in seconds. As the experiments were performed on a pre-existing trail, the concentration profile was set for **Q=1000** and **τ = 300**.

CHAPTER 3

DATA ANALYSIS AND RESULTS

3.1 Model Parameterization

Parameters for the model were defined by characterizing the movement of ants in correlated random walks in an arena with no pheromone (as discussed in Section 2.5.2). In Figure 2.9 it was observed that the trajectories tend to align to the walls of the arena showing the wall following tendency of ants (thigmotaxis [17]). To avoid differences in the behavior of ants caused by the boundary condition, the analysis were done on trajectory bouts that were >1cm from the arena wall.

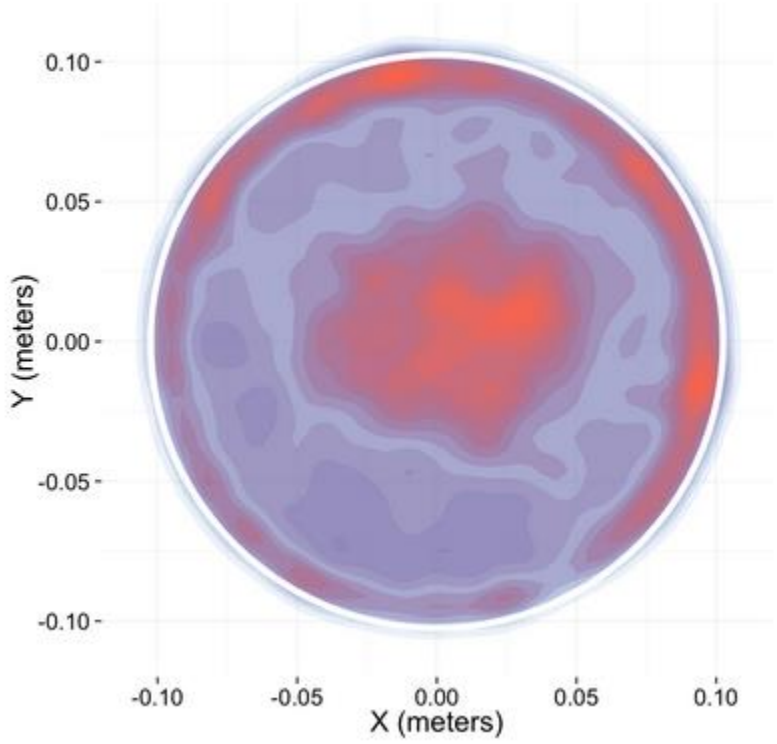

Figure 3.1 Kernel density map shows the distribution of ant locations in the arena during the correlated random walks. Red represents the area with high density of ant locations, and blue represents the area with low density of ant locations. Density of ant locations around the arena wall is high showing thigmotactic tendency.

3.1.1 Linear Speed

The distribution of linear speeds of ants in the arena is shown in Figure 3.2. The mean and median were both seen to be closed to 2cm s^{-1}. Thus, the linear speeds of ants in the simulations were set at 2cm s^{-1} in the model.

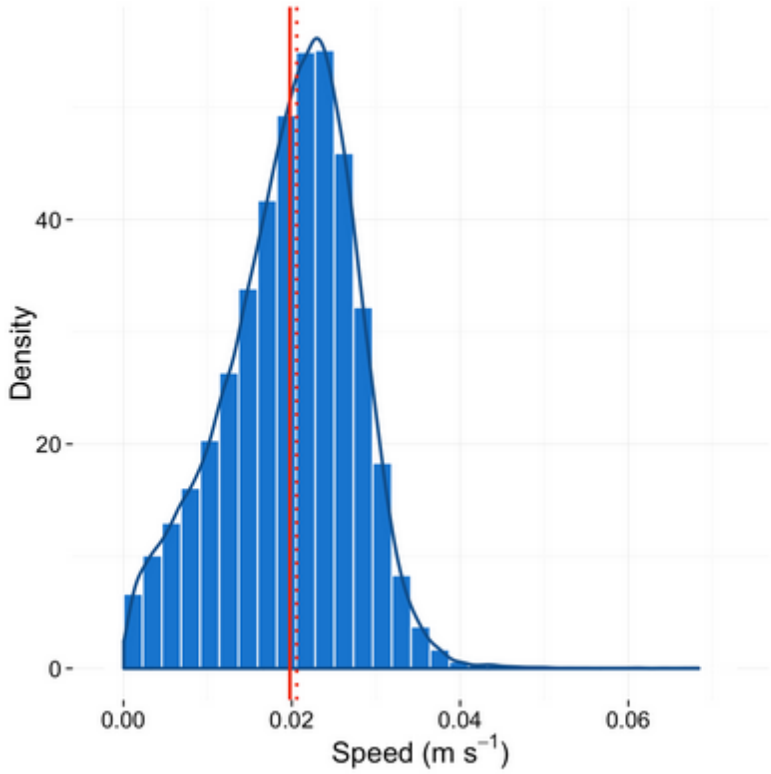

Figure 3.2 Distribution of the linear speeds of the ants in the arena. The mean (plain red line) and the median (dashed red line) were both close to 2cm s^{-1}.

3.1.2 Angular Speed

The angular speeds of ants were measured for linear speeds that are within 1 standard deviation from the average linear speed. This prevents the consideration of extreme cases such as ant stopping or panicking.

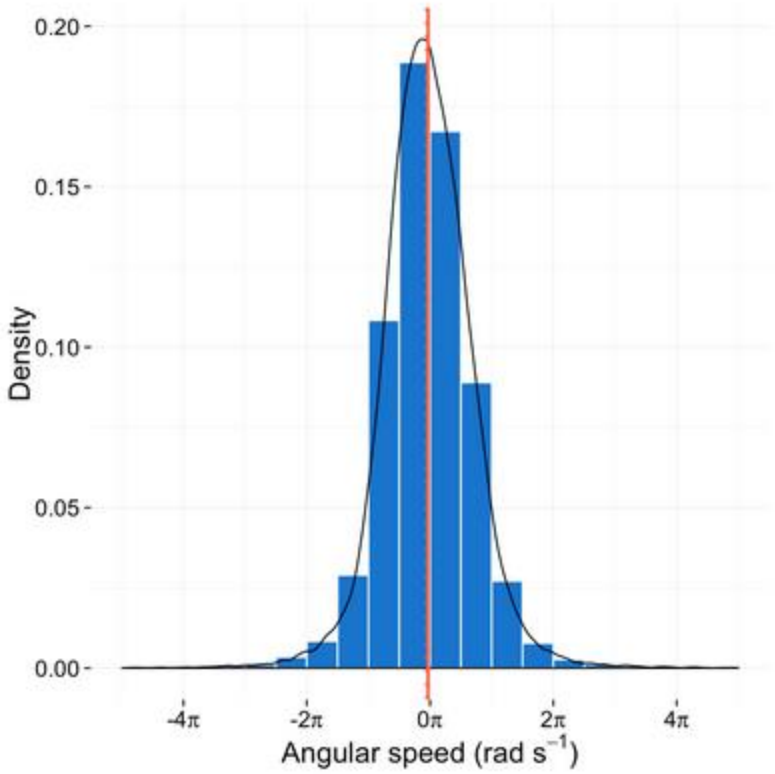

Figure 3.3 Distribution of angular speeds of ants. The mean (plain red line) and median (dashed red line) were all closed to 0 radians.

The distribution of angular speeds is shown in Figure 3.3. The angular speeds were centered around 0 radians with standard deviation of 2.6 radians. This shows that ants are more likely to move straight ahead rather than turning fast between two time steps. The maximum angular speed was calculated as the 95th percentile of the distribution. Maximum angular speed was required for parameter **A** in Weber's Law (equation 1.1), and was set at 4.5 radians.

3.2 Data Preprocessing

3.2.1 Experimental Data

The midline of the trail image was defined by finding its skeleton using the Image Processing tool box in MATLAB® (shown before in Figure 2.6). Ant behaviors were studied by analyzing the ant trajectories around the trail midline. The midline and ant trajectories were plotted for all the runs. The midlines and the trajectories were rotated such that the initial branch falls on the negative X-axis with the branching point coinciding with the origin of the pixel coordinate system (Figure 3.5). The ants either chose the upper or the lower path (emerging branches) after the bifurcation (Figure 3.5).

The trajectories were then standardized such that the end point of each trajectory had a positive Y value (Figure 3.4b). This was done by checking the Y value of the last point of the ant trajectory, which if negative meant the ant chose the lower branch after bifurcation (Figure 3.4a), and hence was flipped upside down (Figure 3.4b).

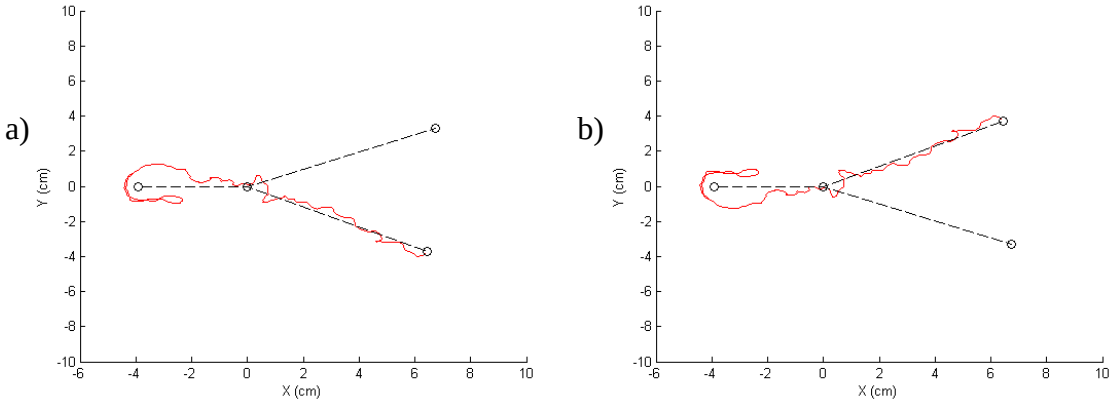

Figure 3.4 a) Midline and the trajectory of the same run as in Figure 2.6. The ant in this run chooses the lower branch after bifurcation. b) The trajectories were flipped such that the ant seems to choose the upper branch. By doing this all trajectories have the same conformation.

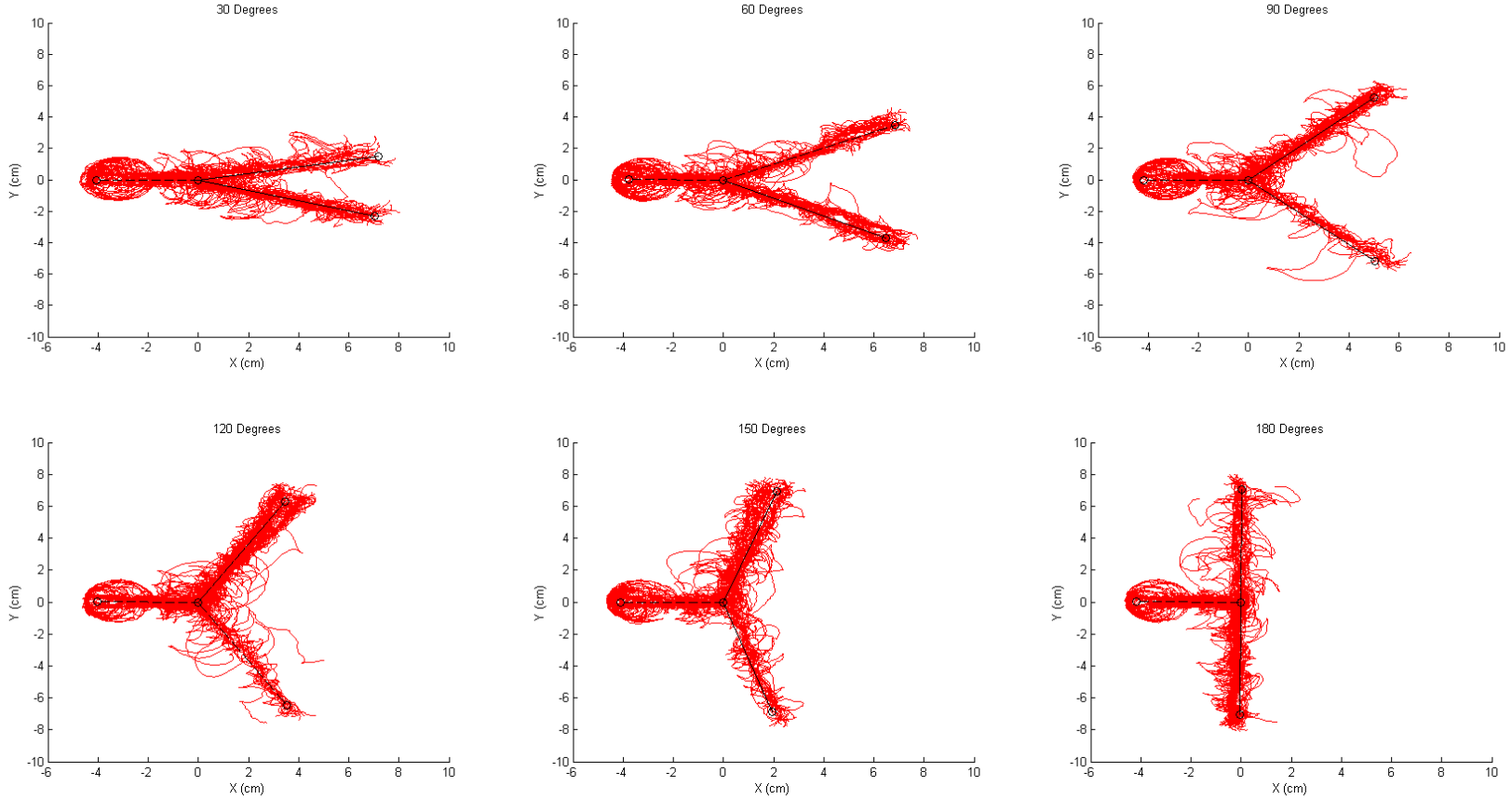

Figure 3.5 Trajectories of ant movement from experiments with different angle of bifurcation (angle of bifurcation can be found on the title of each plot). At the start branch or initial branch, the trajectories tend to coil (thus, a blob of trajectories can be observed at the initial branch) because of the presence of start chamber. The walls of the start chamber enclose the initial part of the start branch along which the ants tend to move because ants exhibit thigmotaxis [17].

3.2.2 Model Data

Figure 3.6 shows the trajectories obtained from the model for the same bifurcation angles as in the experiments.

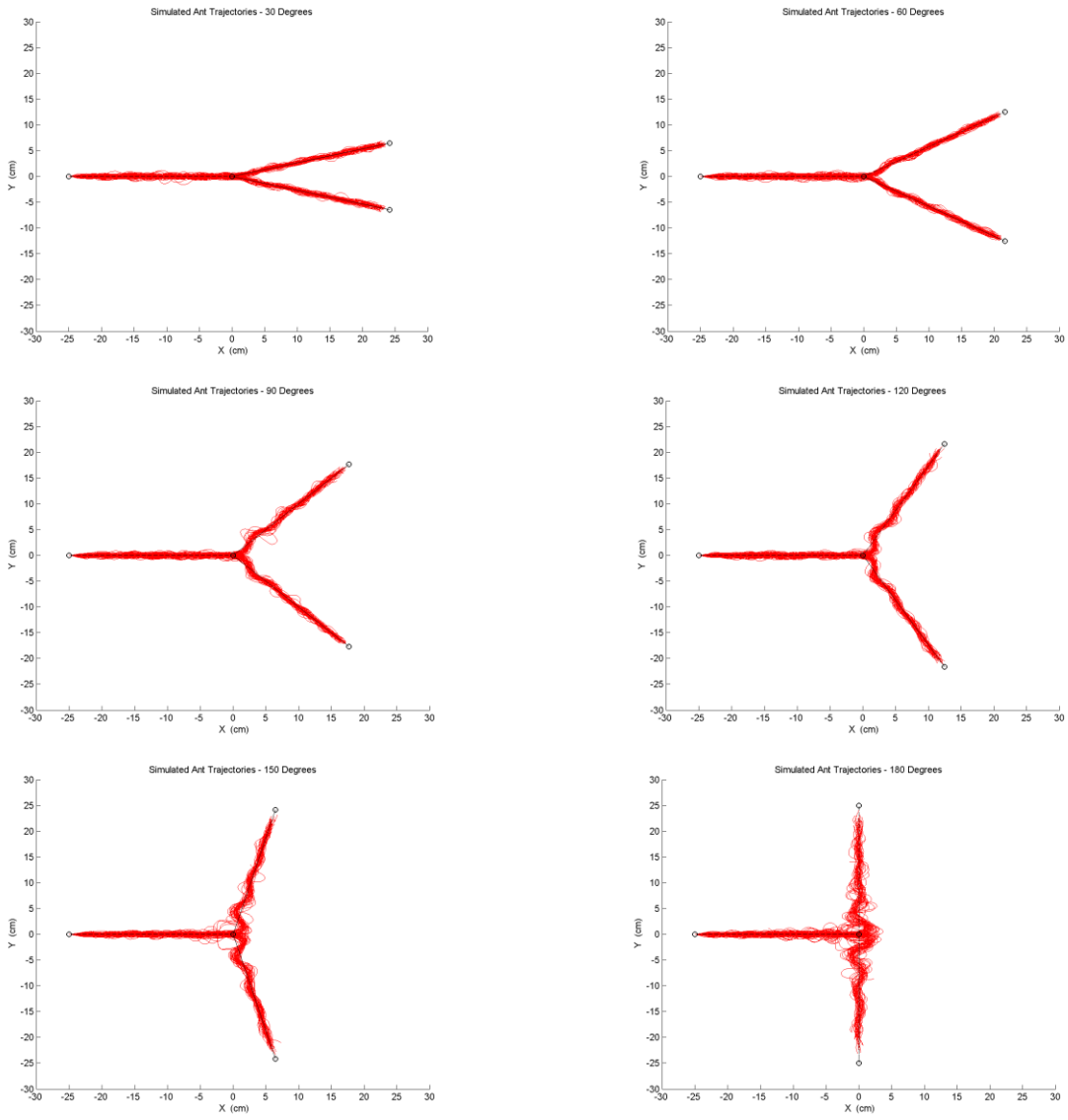

Figure 3.6 Simulated ant trajectories. The corresponding branching angles are as in the title of each plot. The ants can be observed to choose the two branches equally after bifurcation regardless of the bifurcation angle.

Similar to the experimental treatments, the simulated ant trajectories were standardized so that their last position has a positive Y value (Figure 3.7 a and b). The algorithm to standardize data was similar as the one used for experimental trajectories.

a)

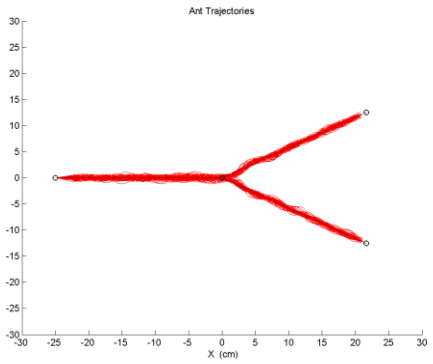

b)

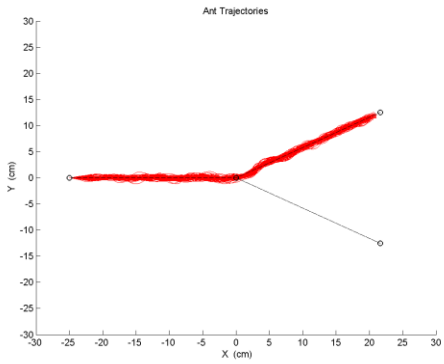

Figure 3.7 a) Simulated trajectories for θ = 60°. b) Trajectories after preprocessing by flipping the trajectories that chose the lower branch.

3.3 Decision Point

The average decision point or the average point where ants decide to choose a branch was measured for each of the standardized trajectories (standardized trajectories of Figures 3.5 and 3.6).

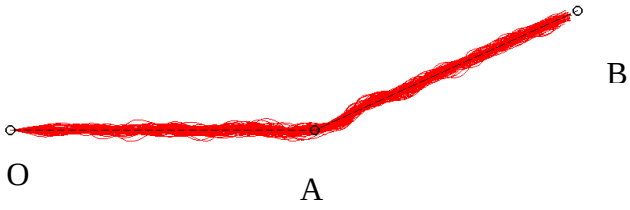

Figure 3.8 OA – Initial Branch; AB – Emerging Branch. Proximity of a point on the trajectory to the initial and emerging branches were compared, based upon which Binary values 0 or 1 were assigned.

To find the average decision point, binary values 0 or 1 were assigned based upon the proximity of a point on the ant trajectory to the two branches OA or AB, respectively (Figure 3.8). In other words, the distances of each point on the trajectory were compared to two segments (i.e., the initial branch OA or the emerging branch AB), where if the point was near the initial branch (i.e., OA) then value 0 was assigned, and if it was near the emerging branch (i.e., AB) then value 1 was assigned. The binary values were plotted against their corresponding X value to which a simplified logistic function was fit of the form:

$$L = \frac{Linf}{1+\exp(-B(X-M))} \tag{1.3}$$

where **L** is the value of the logistic fit at position **X** of the X coordinate. **B** is the rate of growth of the logistic function. **M** is the "Decision point" (i.e., the symmetric inflexion point of the logistic curve). **Linf** is the maximum value of the Logistic function, which is equal to 1 in this case.

3.3.1 Results for Logistic Curve Fit

Figures 3.9 and 3.10 show the Logistic curve fit to the binary values (assigned as per the aforementioned method) for data from the experiments and model, respectively.

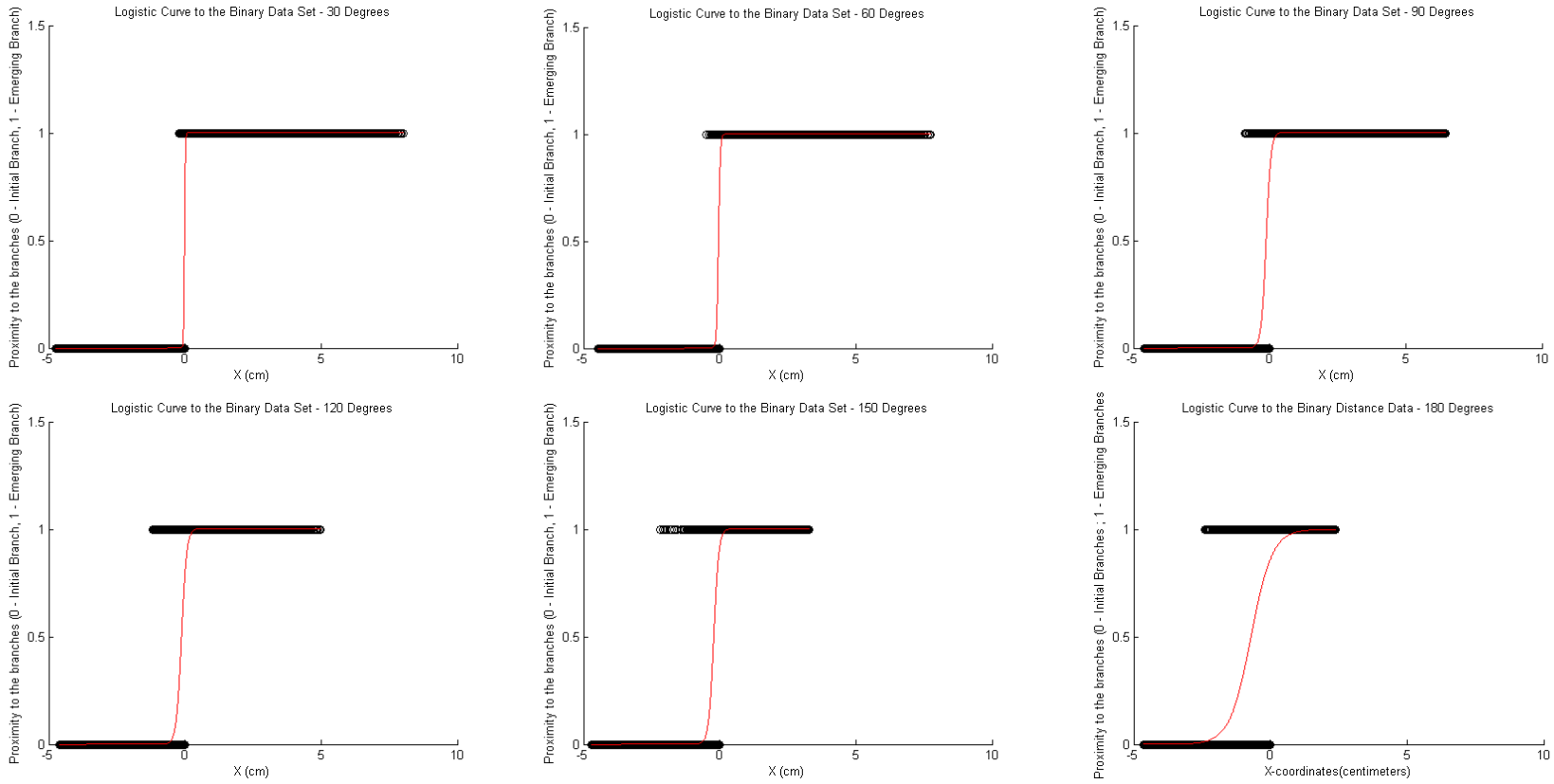

Figure 3.9 Logistic fit to the binary Data (0 or 1) from the ant trajectories extracted from the experiments with differing angle of bifurcations (angle of bifurcation can be found in the title of each plot). The binary values (0 or 1) were assigned based upon the proximity of a point on the ant trajectory to the two branches OA or AB.

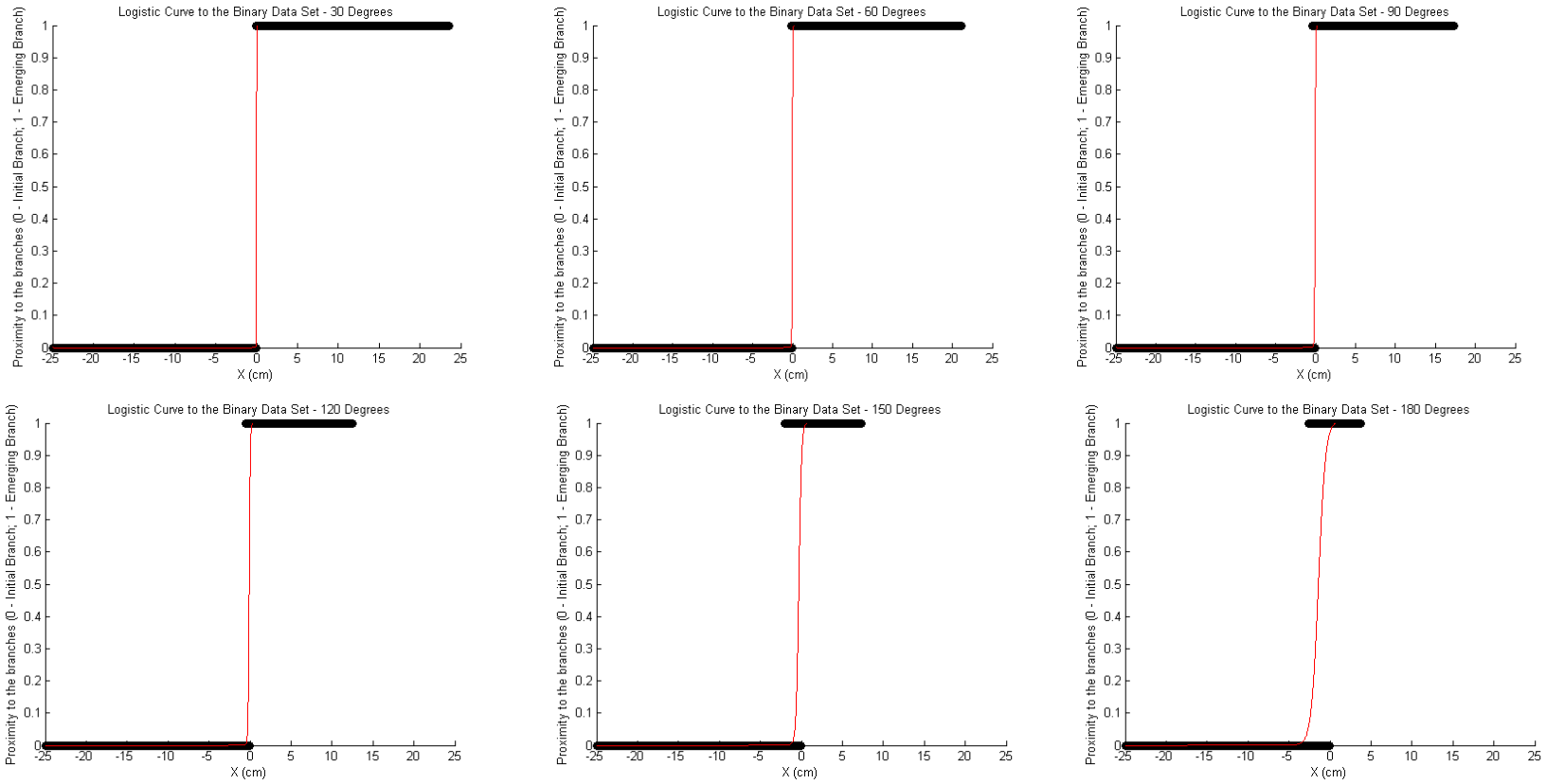

Figure 3.10 Logistic fit to the binary data for the ant trajectories from the model.

The parameters for the above Logistic fits are as shown below:

Table 3.1 Parameter Values of the Logistic Fit for the Experimental Data

Angle of Bifurcation	Decision Point (M)	Maximum Value of Logistic Function (Linf)	Rate of Growth (B)
30 Degrees	-0.0185	1.0000	60.2226
60 Degrees	-0.0464	1.0000	29.4182
90 Degrees	-0.1287	1.0000	11.3608
120 Degrees	-0.1253	1.0000	10.5562
150 Degrees	-0.2172	1.0000	10.8644
180 Degrees	-0.7050	1.0000	2.5733

Table 3.2 Parameter Values of the Logistic Fit for the Simulation Data

Angle of Bifurcation	Decision Point (M)	Maximum Value of Logistic Function (Linf)	Rate of Growth (B)
10 Degrees	-0.0022	1.0000	861.6200
20 Degrees	-0.0081	1.0000	157.8805
30 Degrees	-0.0197	1.0000	68.8418
45 Degrees	-0.0270	1.0000	49.2539
60 Degrees	-0.0356	1.0000	35.0853
90 Degrees	-0.0564	1.0000	25.2204
120 Degrees	-0.1064	1.0000	15.0208
150 Degrees	-0.3096	1.0000	6.0838
180 Degrees	-1.4069	1.0000	2.3223

Table 3.2 shows data for $\theta = 10°$, 20° and 45° provide a better picture of the trends in the results.

3.3.2 Decision Point vs. Angle of Bifurcation (θ)

The decision point can be observed to decrease with an increase in angle of bifurcation in the experimental data, as well as in the model data (column two in Tables 3.1 and 3.2). The trend of the shift in decision points with increasing angle of bifurcation is shown in Figure 3.11.

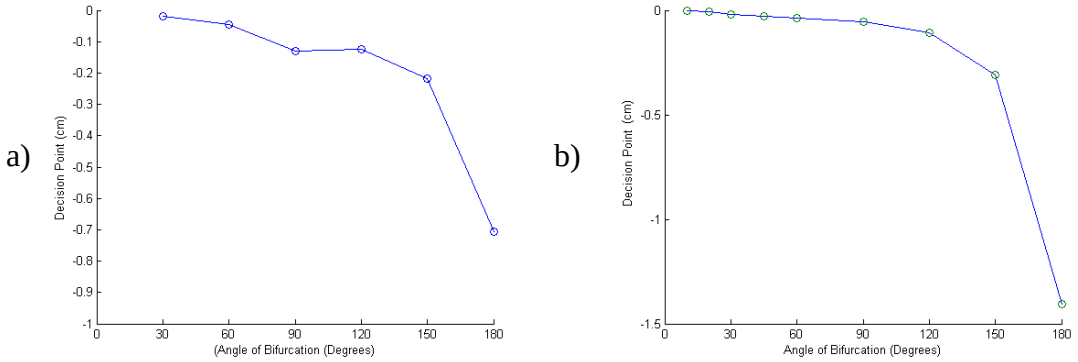

Figure 3.11 Decision point vs. angle of bifurcation plots for a) experimental data, and b) simulation data.

The decision point vs. angle of bifurcation plots for the experimental data and simulation data can be observed to have a similar consensus**.**

3.4 Average Maximum Distance

The average maximum distance was calculated to see how much the angle of bifurcation influences the trail following ability of the ants. This was computed by first calculating the maximum distances of ants in each trajectory (trajectories from experiments and simulations), and then finding the mean (average) of maximum distances of trajectories for each angle of bifurcation. Figure 3.12 shows average maximum distance vs. angle of bifurcation plots for the experimental data and the model data.

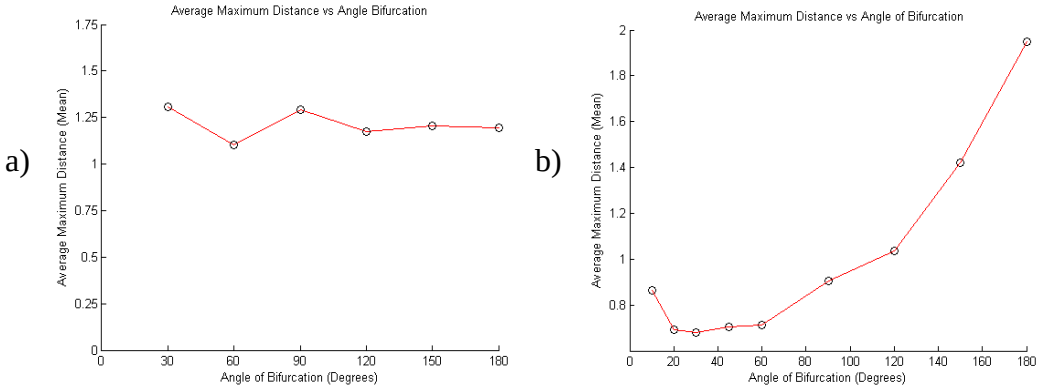

Figure 3.12 Average maximum distance vs. angle of bifurcation (θ) plots for a) experimental data, and b) model data.

The values of the average maximum distance for the experimental data were very random and didn't show any pattern or trend with increasing bifurcation angles (Figure 3.12a). The average maximum distance is observed to increase with increase in angle of bifurcation for the simulation data (Figure 3.12b).

In order to compare the decision points and the average maximum distances, the two values were rescaled between their minimum and maximum values between 0 and 1 such that the minimum value is 0, and the maximum value is 1 (Figures 3.13 a and b).

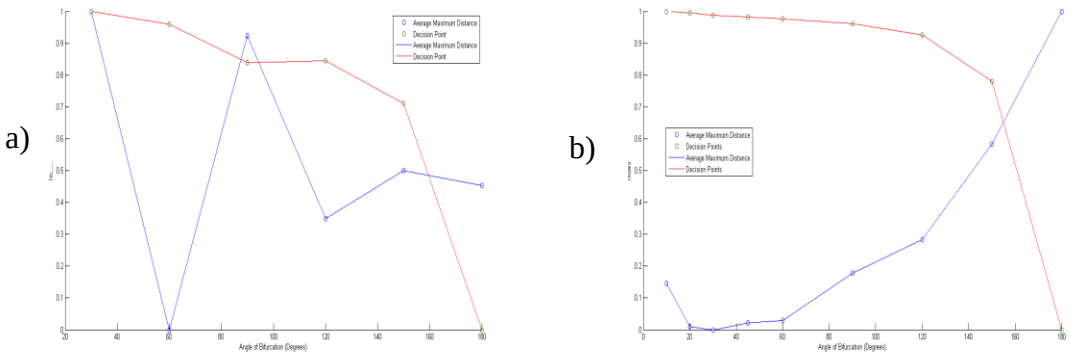

Figure 3.13 Rescaled decision points (red curve) and average maximum distance (blue curve) rescaled and plotted together for a) experimental data, and b) model data.

CHAPTER 4

DISCUSSION

From the logistic plots it can be observed that with an increase in the angle of bifurcation (θ), the decision points move closer towards the initial branch, and thus moves away from the emerging branches. The trend appears to be similar for the data from the experiments and the model (Figure 3.11). Reducing decision point distance means the ants turn earlier in their choice of branch, and since the position of the food source is constant, there will be a decrease in the angle of bifurcation. The results are in accordance with our hypothesis of reducing decision points with increasing angles. Similarly, in the simulation data the average maximum distance can be observed to increase with increase in bifurcation angles (Figure 3.12 b). However, inconsistencies exist between the experiments and the model, which are discussed below. The average maximum distance increases with bifurcation angles in the models because the increase in bifurcation angle makes it difficult for the ant to follow the trail (in Figure 3.4, as θ increases more singular trajectories can be observed to protrude out from the trail) and thus, the chances of ants losing the trail increases. The results of the data from the experiments (Figure 3.12a) disagree with the model, and are discussed below.

In the indexed plot for the model data (Figure 3.13b), both the quantities (decision point and average maximum distance) are at minimum when θ is between 20° and 60°. These are the points where there is a compromise between the decision points and average maxima values. An ant network with the above degree of bifurcations will have constant network architecture as the decision points remain close to 0 (parameter **M** from Table 3.2 i.e., the ants make their decision to choose an emerging branch almost at the

bifurcation). Low average maximum distance means the ants follow the trail well, and thus the chances of ants losing the trail are also reduced.

The general trends of results for decision points are similar in the experimental and the model data, but a small deviation exists between the two data sets, for example there is a slight increase in decision points for values of θ from 90° to 120°. The reason for this deviation might be due to lower number of replicates in the experiments. Any collective behavior or pattern of an ant colony initially shows a stage of fluctuation that settles with time and increasing number of ants. *L. humile* traffic rate can become superior to 10 ants per second (personal communication with Simon Garnier), as a result the number of experimental replicates correspond to the 7-8 seconds of the colony foraging time. This time is too low for an ant colony to shape a trail network and show a foraging pattern.

The average maximum data for the experimental runs were very irregular, and were in complete discordance with the hypothesis and with the results from the simulations. The main reason for this discordance can be attributed to the experimental procedures in which the runs were conducted. Figure 4.1 shows the distribution of pheromone around the trail in the simulation and in the natural setup, where pheromone has highest concentration at the middle of the trail, and then reduces with the increase in radial distance.

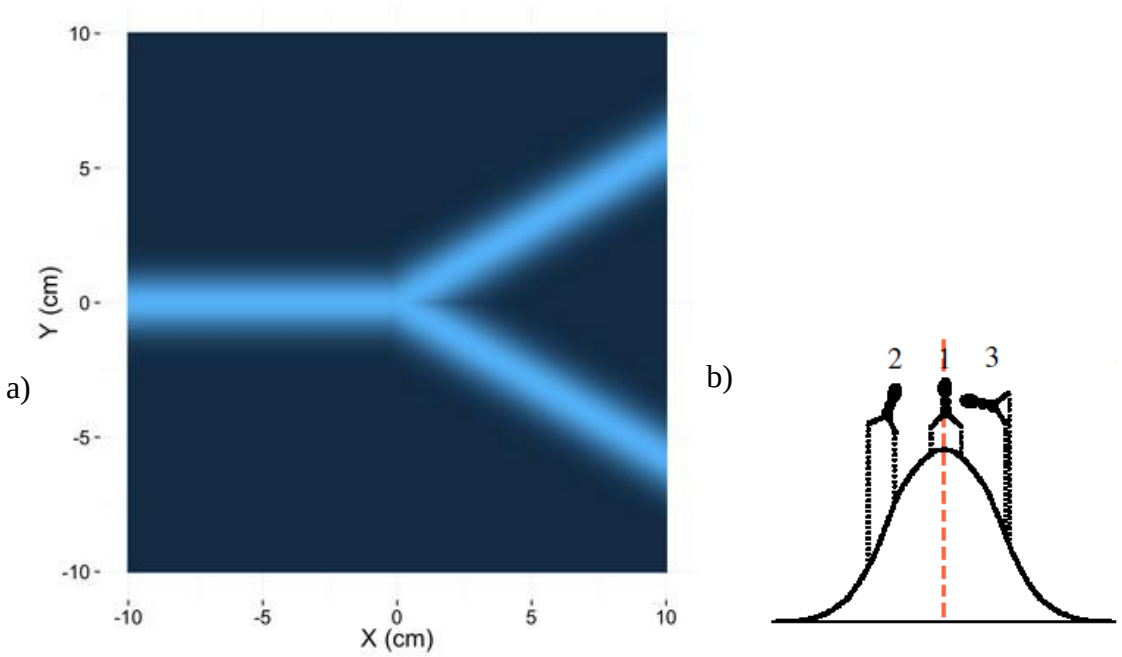

Figure 4.1 a) Pheromone concentration profile of the trail model. b) Cross section view of the pheromone concentration profile of the trail, where, the angle of an ant relative to the pheromone trail influences its ability to determine concentration gradients correctly [18].

In the experimental setup, pheromone strips were used where it might be speculated that the strips didn't have the same pheromone concentration profile as shown in Figure 4.3a. This may be because, firstly, the exact areas where pheromones were deposited are unknown. When marking the pheromones strips in a different setup, there were certain areas where ant traffic flow was higher, and certain places where it was lower. Also, ants leave pheromone both when moving out of the nest in search for food and when going back to the nest in recruitment [19] as well as during exploration [20]. However, the qualities of pheromone might differ in each of the cases (especially when leaving the nest for the food source and when coming back to the nest). As a result, defining the correct pheromone profile of the paper strips becomes difficult. Secondly, the pheromone paper strips were marked by ants in a completely different setup from

where the paper strips were removed, rearranged and then used in the experimental runs. In this process, the pheromone concentration might be reduced abruptly in the part of the arena adjacent (radially) to the paper strips as the diffusion of pheromone is not continuous and thus, fails to follow a Gaussian concentration profile (Figure 4.2). In such a pheromone concentration profile, a slight change in the relative angle of the ant might result in ant leaving the trail (Figure 4.2).

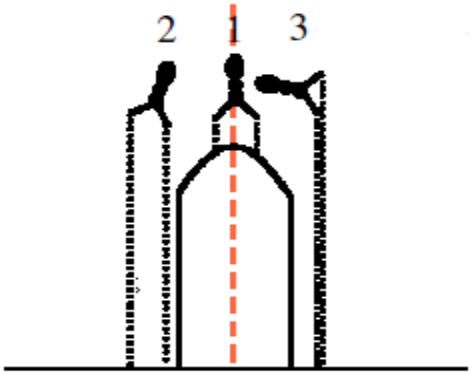

Figure 4.2 Pheromone concentration profile in the marked paper strips (used in the experiments). If the ants move straight or at a narrow angle with respect to the trail, then ants will continue to walk on the trail (ant 1 – in the figure), if there is a significant change in the relative angle (ant 2 and ant 3) the ant may lose the trail.

Synthetic pheromones ((Z)-9-hexadecenal) may be one of the option to study individual ant responses to trail pheromones [19, 21]. This approach allows control over concentrations gradients, but fails to produce the physical and physico-chemical properties of the trails. (Z)-9-hexadecenal is the active compound of *L. humile* trail pheromone, which is 200 times less active when presented alone than in the form of ant gaster extracts with an equivalent amount of active molecule [19]. It is also difficult to relate the concentration of synthetic pheromones to the actual concentration present in the trails. Thus pheromone paper strips were preferred over the synthetic pheromone in this study.

It is necessary for ant colonies to form efficient trail networks to exploit and forage for food sources. In earlier studies it has been found that the efficiency of an ant trail network lays in the geometry of the trail bifurcations i.e., in the angle of bifurcation [4-7]. A network can be considered efficient if the ants follow the trail smoothly, and the structure remains stable with time. The results show that these constraints are met when the angle of bifurcation (θ) ranges between 20° and 60°. For θ within this range, the average maximum distance of the ants is low, meaning ants profusely follow the trail, thereby reducing the chances of ants losing the trail. Moreover, the decision points for the ants at these bifurcating angles are close to zero, meaning the ants decide to turn towards one of the branches almost at the bifurcation itself. This means that the structure remains stable with time and the passage of more ants performing the same dynamics (as deviations in the decision point from the bifurcation point might result in an increase or decrease in the angle of bifurcation).

REFERENCES

1. Hölldobler B, and Wilson EO, *The ANTS*. 1990: The Belknap Press of Harvard University Press.

2. Oster GF, Wilson EO, *Caste and ecology in the social insects*. 1978, Princeton University Press.

3. Hölldobler B, and Möglich M, *The foraging system of Pheidole militicida (Hymenoptera: Formicidae).* Insectes Sociaux, 1980. **27**(3): p. 237-264.

4. Acosta FJ, López F, and Serrano JM, *Branching Angles of Ant Trunk Trails as an Optimization Cue.* Journal of Theoretical Biology, 1993. **160**(3): p. 297-310.

5. Garnier S, Guérécheau A, Combe M, Fourcassié V, Theralauz G, *Path selection and foraging efficiency in Argentine ant transport networks.* Behavioral Ecology and Sociobiology, 2009. **63**(8): p. 1167-1179.

6. Gerbier, G, Garnier S, Rieu C, Theralauz G, Fourcassié V, *Are ants sensitive to the geometry of tunnel bifurcation?* Animal Cognition, 2008. **11**(4): p. 637-42.

7. Vittori K, Talbot G, Gautrais J, Fourcassié V, Araujo AF, Theralauz G, *Path efficiency of ant foraging trails in an artificial network.* Journal of Theoritical Biology, 2006. **239**(4): p. 507-15.

8. Jackson DE, Holcombe M, and Ratnieks FL, *Trail geometry gives polarity to ant foraging networks.* Nature, 2004. **432**(7019): p. 907-9.

9. Buhl J, Hicks K, Miller ER, Persey S, Alinivi O, Sumpter DJ, *Shape and efficiency of wood ant foraging networks.* Behavioral Ecology and Sociobiology, 2008. **63**(3): p. 451-460.

10. Bhatkar A, and Whitcomb WH, *Artificial Diet for Rearing Various Species of Ants.* The Florida Entomologists, 1970. **53**.

11. Deneubourg JL, Aron S, Goss S, Pasteels JM, *The self-organizing exploratory pattern of the argentine ant.* Journal of Insect Behavior, 1990. **3**(2): p. 159-168.

12. Lochmatter T, Roduit P, Cianci C, Correll N, Jacot J, Martinoli A, *SwisTrack - a flexible open source tracking software for multi-agent systems.* 2008: p. 4004-4010.

13. Perna A, Granovskiy B, Garnier S, Nicolis SC, Labedan M, Theralauz G, Fourcassié V, Sumpter DJ, *Individual rules for trail pattern formation in Argentine ants (Linepithema humile).* PLoS Computational Biology, 2012. **8**(7): p. e1002592.

14. Calenbuhr V, Deneubourg JL, *A model for osmotropotactic orientation (II).* Journal of Theoretical Biology, 1992. **158**(3): p. 395-407.

15. Calenbuhr V, and Deneubourg JL, *A model for osmotropotactic orientation (I).* Journal of Theoretical Biology, 1992. **158**(3): p. 359-393.

16. Evershed RP, Morgan ED, and Cammaerts MC, *3-ethyl-2,5-dimethylpyrazine, the trail pheromone from the venom gland of eight species of Myrmica ants*. Insect Biochemistry, 1982. **12**(4): p. 383-391.

17. Dussutour A, Deneubourg JL, and Fourcassié V, *Amplification of individual preferences in a social context: the case of wall-following in ants.* Proceedings of Biological Science, 2005. **272**(1564): p. 705-14.

18. Couzin ID, and Franks NR, *Self-organized lane formation and optimized traffic flow in army ants.* Proceedings of Biological Sciences, 2003. **270**(1511): p. 139-46.

19. Van Vorhis Key SE, and Baker TC, *Observations on the trail deposition and recruitment behaviors of the argentine ant, Iridomyrmex humilis (hymenoptera: formicidae).* Annals of the Entomological Society of America, 1986. **79,**: p. 283-288(6).

20. Aron S, Pasteels JM, Deneubourg JL, *Trail-laying behaviour during exploratory recruitment in the argentine ant, Iridomyrmex humilis (mayr).* Biology of Behavior, 1986: p. 207-217.

21. Suckling DM, Peck RW, Manning LM, Stringer LD, Cappadonna J, El-Sayed AM, *Pheromone disruption of Argentine ant trail integrity.* Journal of Chemical Ecology, 2008. **34**(12): p. 1602-9.